Science and Technology Indonesia
e-ISSN:2580-4391 *p*-ISSN:2580-4405
Vol. 10, No. 4, October 2025

Research Paper

MgO Scattering Effects on CCT Uniformity and Lumen Strength of The Traditional White LED Packages

Pham Van De[1], Dang Truong Thinh[2], Sang Dang Ho[2*]

[1]*Faculty of Engineering, Dong Nai Technology University, Dong Nai Province, 76000, Vietnam*
[2]*Power System Optimization Research Group, Faculty of Electrical and Electronics Engineering, Ton Duc Thang University, Ho Chi Minh City, 70000, Vietnam*
***Corresponding author**: hodangsang@tdtu.edu.vn

Abstract
Scattering of light within white light-emitting diodes (LEDs) is crucial for minimizing internal reflection and ensuring consistent color distribution. Among the array of scattering-induced nanoparticles, magnesium oxide (MgO) stands out for its distinctive scattering performance, positioning it as a promising material in the field of optic fiber sensing. This study investigates the integration of MgO nanoparticles into yellow phosphor films with the aim of augmenting the color uniformity and luminous efficiency of conventional white LEDs, specifically those excited by blue light. Light scattering is evaluated across varying concentrations of MgO within the phosphor layer. Results reveal that manipulation of MgO nanoparticle concentration enables precise control over correlated color temperature (CCT) regulation in white LEDs. Furthermore, the inclusion of MgO nanoparticles reduces the requisite amount of yellow phosphor for LED fabrication, thereby curbing production costs. Significantly, MgO exhibits potential in harmonizing CCT and luminosity in white LEDs. Additionally, there is a marginal improvement in color quality scale with increasing MgO concentration. The optimal MgO concentration for achieving a balance between CCT uniformity, luminosity, and color reproduction parameters is determined to be 7 wt.%.

Keywords
MgO, YAG:Ce^{3+}, LEDs, Lumen Output, Color Quality

Received: 3 February 2024, Accepted: 4 September 2024
https://doi.org/10.26554/sti.2025.10.4.1280-1287

1. INTRODUCTION

White light-emitting diodes (LEDs) have emerged as a cornerstone in general lighting applications owing to their remarkable luminous efficiency, vibrant color rendition, cost-effectiveness, and extended operational lifespan (Cong and Anh, 2025; Chen et al., 2021). Presently, the prevailing methodology for achieving white light in LEDs involves combining the blue emission from the LED die with the excited emission from a phosphor material. Despite significant advancements in phosphor-converted white LED technology, the quest for enhancing luminous efficacy persists as current achievements still fall short of theoretical limits (Anh et al., 2025; Dawodu et al., 2020). Over the past decade, luminous efficacy has nearly doubled; however, considerable headroom remains for improvement, particularly through enhancements in blue-chip and package efficiency, as well as spectral efficiency via the development of fluorescent materials possessing optimal optical characteristics and high photoluminescence (Du et al., 2020; Fuertes et al., 2019). Notably, challenges persist in ensuring high-quality white light output from LEDs, impeding their widespread adoption in advanced solid-state lighting systems (Huang et al., 2021). Key issues plaguing conventional white LEDs include insufficient internal light scattering, which leads to pronounced total internal reflection and phosphor self-absorption, alongside inferior angular correlated color temperature distribution (Huang et al., 2021). Addressing these challenges necessitates innovative strategies. One such strategy involves the incorporation of nanoparticles (NPs) into silicone encapsulation, proving to be a straightforward and effective means of enhancing the luminosity of blue LEDs. Extensive research has explored materials like SiO_2, TiO_2, and ZnO, demonstrating promising results in boosting the luminous efficiency of blue-pumped white LEDs (Thi et al., 2020b). Among these materials, MgO nanoparticles have garnered significant attention due to their exceptional biocompatibility, non-toxicity, robust stability in diverse environmental conditions, and wide-ranging applications, particularly in biomedicine (Anh and Ngoc, 2020). MgO distinguishes itself among non-magnetic oxide systems as a pivotal material in various technological domains, attributed to its simple crystal structure and absence of d orbital elec-

trons, which facilitate comprehension of its diverse physical and chemical behaviors. MgO has been utilized to enhance the thermo-control performance of Al_2O_3 coatings and improve the light transmittance of Al_2O_3-coated ceramics (Thi et al., 2020a). Furthermore, its high-scattering characteristics have been harnessed to amplify the backscattering strength of fibers for high-performance optical fiber sensors (Jones et al., 2021), along with enhancing the conversion performance of phosphor materials in phosphor films, thereby augmenting LED luminous flux (Jost et al., 2018).

This study focuses on incorporating MgO nanoparticles into yellow phosphor films to enhance the color uniformity and luminous efficiency of conventional blue-excited white LEDs. The sol-gel synthesis is utilized for the nanoparticle preparation, offering advantages such as higher product yields, straightforward procedures, and minimal temperature requirements (Jost et al., 2018). The scattering of light is evaluated across various concentrations of MgO in the phosphor layer utilizing the Mie scattering theory. This paper is structured as follows: Section 2 outlines the methods employed for preparing MgO nanoparticles and MgO-doped phosphor layers. In Section 3, the equations utilized for calculating optical scattering and discussions on the obtained LED performances are presented. Finally, Section 4 encapsulates the research findings, offering insights for future investigations and applications of MgO to enhance phosphor-converted LED lighting performance. Preliminary results demonstrate that adjusting MgO nanoparticle concentration enables control over correlated color temperature regulation, while effectively improving CCT uniformity and reducing the amount of yellow phosphor, thereby contributing to cost reduction in LED production.

2. EXPERIMENTAL SECTION

2.1 Materials

The experimental synthesis of magnesium oxide (MgO) nanoparticles utilized high-purity reagents to ensure the integrity and reproducibility of the results. Oxalic acid dihydrate (>98% purity) and magnesium acetate tetrahydrate (99.5% purity) were sourced from Merck, while methanol (99.9% purity) served as the solvent in the synthesis process. Fluorescence lifetime measurements were conducted using a FLS980 fluorescence spectrometer from Edinburgh, providing insights into the temporal behavior of the emitted light. Assessment of light scattering within the phosphor layer was achieved through a light distribution tester, featuring a 10 cm diameter integrating sphere, rotating table, and 410-660 nm laser sources, enabling detailed examination of scattering phenomena. The color performance of the resulting white LED assemblies was evaluated using a PMS-80 fluorescence spectrum analysis system from Everfine, operating within the 380-800 nm wavelength range, thereby facilitating precise characterization of spectral properties. All experiments were conducted under ambient conditions to ensure consistency and reproducibility. To simulate the effects of nanoparticles on white LED properties, Mie-theory-based simulations were performed using a MATLAB program.

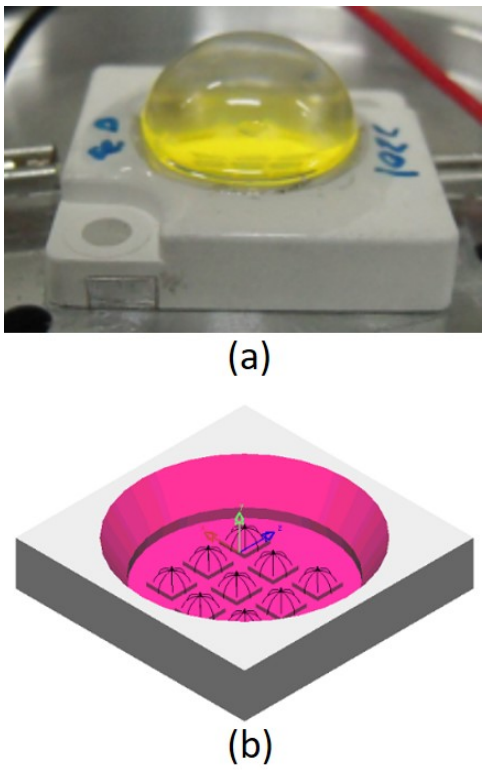

Figure 1. The LED Model Illustration: An Actual White LED (a), White-LED Simulation Created with Light Tools Software (b)

2.2 Preparation

The synthesis of magnesium oxide nanoparticles involved a multi-step procedure to ensure the formation of high-quality crystalline structures. Initially, magnesium acetate tetrahydrate was dissolved in methanol and stirred until a clear solution was obtained. The pH of the solution was then adjusted to 5 using 0.1 M oxalic acid, resulting in the formation of a white gel upon vigorous stirring. After allowing the gel to undergo further gelation for 12 hours, it was dried in an oven at 200°C for 24 hours to remove any residual solvent and facilitate solidification. The resulting solid was subsequently crushed and sieved to obtain a fine magnesium oxalate complex powder, which was subjected to calcination at 950°C for 6 hours in a furnace to yield MgO nanoparticle crystals with desired properties (Lee et al., 2018). The white LED model employed in this study utilized a specially formulated MgO nanoparticles in conjunction with YAG:Ce^{3+} yellow phosphor and a series of blue LED die emitting at 465 nm. Figure 1 illustrates the configuration of the white LED apparatus, providing both a physical depiction (Figure 1a) and a 3D simulation model generated using LightTools software (Figure 1b). The simulation setup incorporated a blue LED die positioned at the base, with a conformal converter encapsulant situated atop a reflector cup.

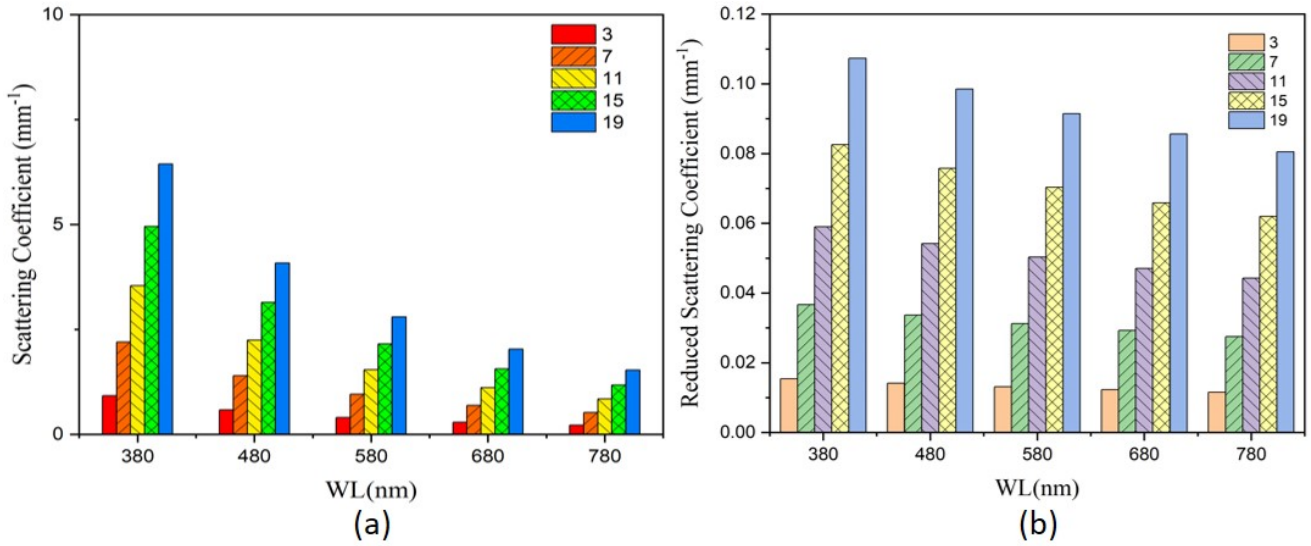

Figure 2. Scattering Coefficients (a) and Reduced Scattering Coefficients (b) of MgO Nanoparticles with Different Weight Concentrations from 3 wt.% to 19 wt.%

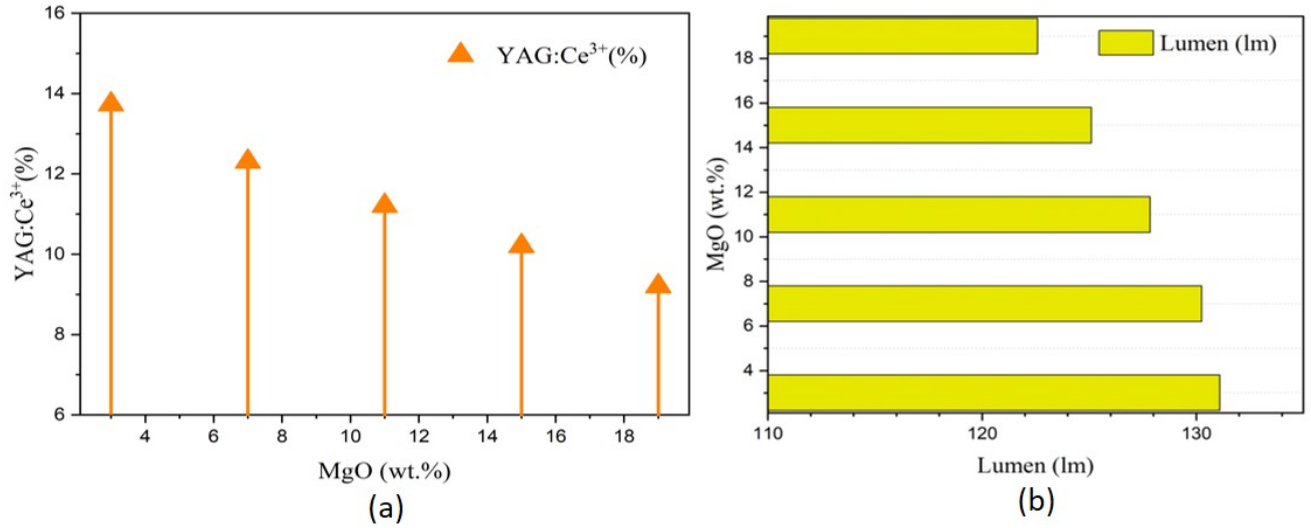

Figure 3. Changes in YAG:Ce^{3+} (a) and Lumen Output (b) with Different MgO Concentrations

Radiant properties of both the blue LED and the converted light from the yellowish-emitting phosphor were captured by a hemispherical detector positioned at a radial distance of 60 mm from the chip's center. The blue LED die, with dimensions of 0.65 mm × 0.65 mm and a height of 0.1 mm, resided atop a silicon substrate measuring 0.69 mm × 0.69 mm. The reflector cup featured a bottom length of 1.47 mm, a height of 0.5 mm, and a top length of 2.18 mm.

3. RESULTS AND DISCUSSION

3.1 The Scattering of MgO in the Phosphor Layer

The scattering in the phosphor layer is assessed with the reduced scattering coefficient δ_{sca}, as can be computed as follows Li et al. (2018a):

$$\delta_{sca} = \mu_{sca}(1 - g) \quad (1)$$

where μ_{sca} indicates the scattering coefficient, and g denotes the anisotropy factor. The calculated δ_{sca} is depicted in Figure 2, with Figure 2a and Figure 2b depicting the scattering coefficients and reduced scattering coefficients of MgO nanoparticles,

Table 1. Result Comparison of Scattering Coefficients Influenced by Particle Sizes of Scattering Materials

Scattering Materials	Scattering Coefficients (mm^{-1})	Reduced Scattering Coefficients (mm^{-1})	References
SiO_2	7.2	0.78	(Le et al., 2024)
TiO_2	129.4	39.3	(Anh and Lee, 2024)
ZnO	133.9	11.4	(Tung et al., 2024a)
$CaCO_3$	8.96	0.15	(Tung et al., 2024b)
MgO	2.2	0.37	This work

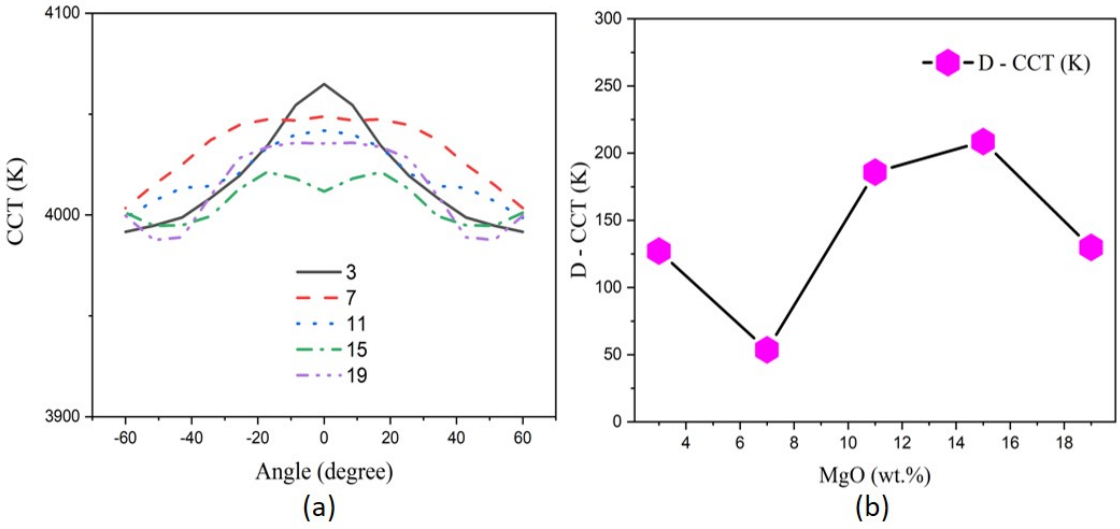

Figure 4. The CCT Angular Distribution (a) and CCT-Deviation (b) With Different MgO Contents

respectively. It is known that the scattering coefficient can determine optical proficiency in WLED apparatuses by boosting dispersion activities, thus boosting consistency for illumination allocation as well as chroma. Regardless, immoderate values of said element may end up lessening lumen since illumination would be confined or guided ineffectively. Notably, shorter wavelengths exhibited more pronounced scattering within the phosphor layer compared to longer wavelengths. Furthermore, higher concentrations of MgO corresponded to improved δ_{sca} values, indicating enhanced utilization of blue radiation to augment phosphor conversion and emission. This heightened scattering of re-emitted light by the phosphor layer played a pivotal role in achieving more uniform color coordination, effectively mitigating angular correlated color temperature (CCT) variance (Li et al., 2018a). The aforementioned findings were gathered from the study and compared to our previous research on related topics that involved LED devices tested with luminescent phosphors to improve optical performance and other metal oxides. The luminous phosphor $KBaYSi_2O_7$: Bi^{3+}, Eu^{3+} is employed in the first paper used for comparison (Loan et al., 2024), whilst metal oxide ZnO is used in the second (Cong et al., 2024). The scattering coefficient results under the influence of MgO are comparable to those of the two compared investigations, as shown by the compared data in Table 1 (Le et al., 2024; Anh and Lee, 2024; Tung et al., 2024a; Tung et al., 2024b).

Additionally, Figure 3 exhibits the influence of MgO on certain optical attributes. The incorporation of MgO resulted in significant savings in phosphor usage, as evidenced by Figure 3a. If integrated into YAG:Ce phosphor sheets, MgO augments illumination dispersion because of significant refraction index. Said dispersion augments angle chroma consistency for generated illumination, ensuring sight consistency under disparate beholding angles. Higher MgO concentrations correlated with reduced quantities of YAG:Ce phosphor, indicating a decrease in self-absorption-induced light loss and subsequent enhancement of converted light extraction from the phosphor layer. Notably, the MgO presence should see proper regulation, since immoderate quantities lessen lumen due to an illumination portion being confined or assimilated unto phosphor sheets. Consequently, this optimization strategy stands to bolster the overall luminous efficiency of the white LED, underscoring the multifaceted benefits of MgO integration in phosphor-converted LED lighting systems (Yang et al., 2021; Loan et al., 2024; Zhang et al., 2017).

Table 2. Comparative Tables of This Research Results with Reported Research

Scattering Materials	CCT (K)	D-CCT (K)	CRI	CQS	Lumen (lm)	References
SiO_2	3000	30	56.3	42.5	73.7	(Le et al., 2024)
TiO_2	4000	49.6	54.5	63.3	125.7	(Anh and Lee, 2024)
ZnO	4000	75	57.9	64.7	126	(Tung et al., 2024a)
$CaCO_3$	6000	460	60.8	62.6	173.2	(Tung et al., 2024b)
MgO	4000	53.6	57.2	63.6	130.3	This work

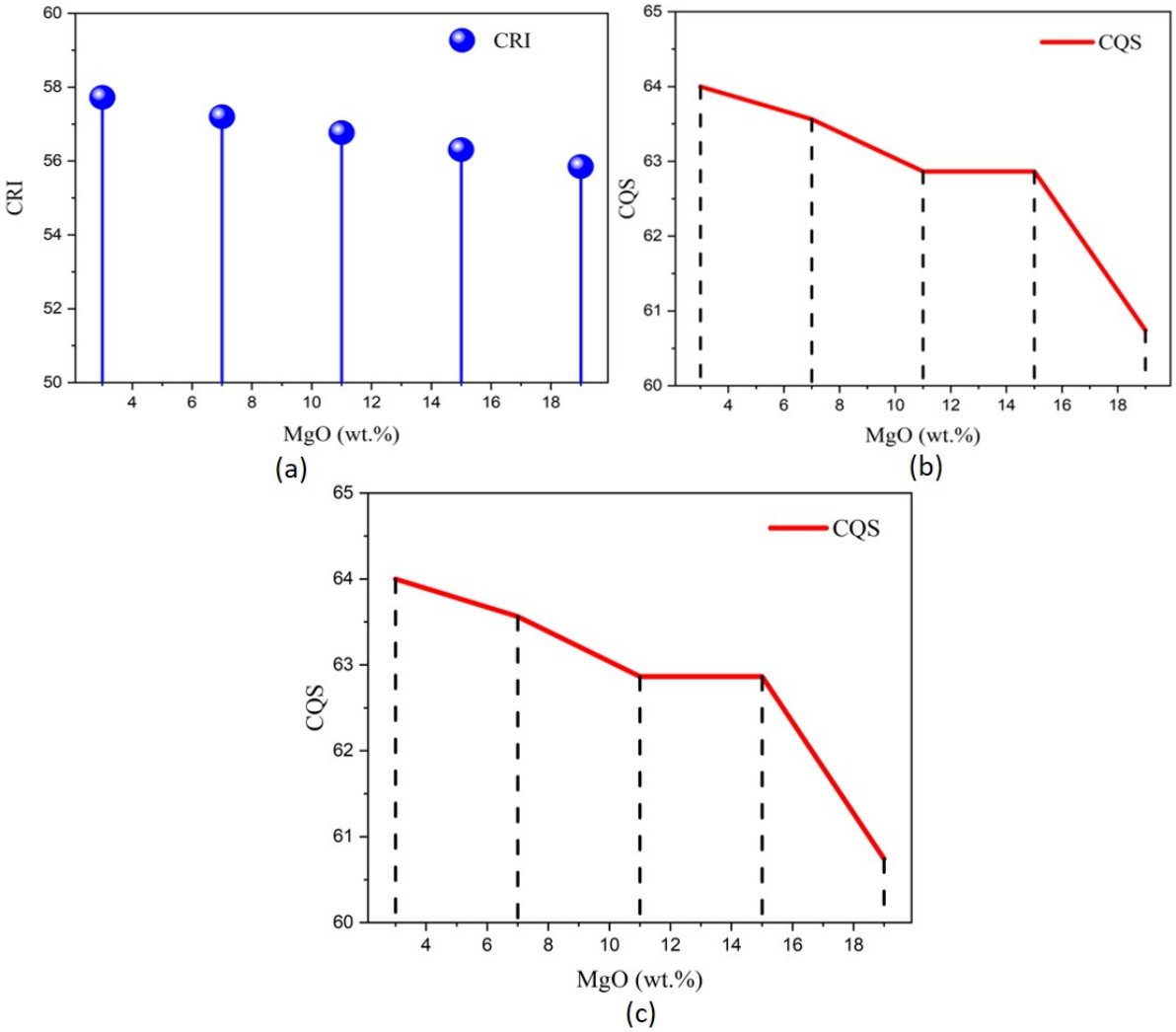

Figure 5. CRI Values (a), CQS Values (b) and (c) Spectra Values with Different MgO Contents

3.2 Effects of MgO with Varying Concentration on White-LED Properties

To elucidate the impact of MgO concentration on the lumen strength of white LEDs, Figure 3b provides further information. Contrary to the assumption that increasing MgO content would enhance lumen output, the lumen reduces gradually as the MgO content become larger. Higher MgO concentrations intensify scattering within the phosphor layer, resulting in light undergoing more random walks rather than following a straightforward path. This increased scattering leads to multiple encounters with the phosphor, where light is absorbed and reemitted, gradually diminishing its energy after each event (Loan et al., 2022; Zhong et al., 2019). Consequently, lumen output declines, exacerbated by potential backscattering phenomena induced by intensified scattering. If MgO concentration is not properly controlled, it will lead to unneeded

dispersion, thus degrading lumen proficiency. Notably, the decline in luminosity is more pronounced with higher concentrations of MgO, highlighting the intricate balance required to mitigate the adverse effects of backscattering while regulating scattering to achieve reduction in CCT variance. The data suggests that MgO concentrations within the range of 3-10 wt.% are appropriate for mitigating the severe impact of backscattering while optimizing CCT-variance reduction (Li et al., 2018b).

Figure 4 exhibits the influence of MgO on the CCT angular distribution and CCT-deviation. Figure 4a presents the angular CCT performance of LEDs with varying MgO concentrations, supported by computed CCT variance data in Figure 4b. On the other hand, MgO generates redshift within the discharge spectrum, altering CCT levels in the WLED apparatus. Said shift lessens CCT, generating a needed warmer illumination hue. The angular CCT values closely mirror variations in lumen output. At 3 wt.% MgO, the highest light intensity at the center produces an upward-cone shape, indicative of intense light output. However, beyond 3 wt.% MgO, both CCT levels and center intensity decrease, signaling a decline in forward-extracted light intensity and subsequently, lumen output. This phenomenon can be attributed to the scattering effect of MgO, where low MgO concentrations favor dominant forward transmission, while higher concentrations gradually smooth out scattered light intensity (Li et al., 2018a; Ma et al., 2021; Peng et al., 2018). Once again, managing MgO concentration proves paramount, since immoderate concentration yielding unnecessary dispersion, influencing CRI and CQS (Anh and Lee, 2024).

The relationship between CCT uniformity and lumen output is explored to address the challenge of balancing light quality and intensity. Figure 4b illustrates the CCT variance with different MgO concentrations, revealing significant fluctuations among specific concentrations. Lesser MgO particle sizes disperse lesser illumination wavelength levels, thus yielding chiller hues under 1 wt.%. It shows relatively substantial decline when the particle size surges to 7 wt.%, which would yield warmer hues, before showing a conversely large surge beyond said particle size. Notably, the CCT variance reaches its lowest point at 7 wt.% MgO, indicating optimal balance between CCT uniformity and lumen intensity. Conversely, a peak in CCT variance is observed at 15 wt.% MgO, underscoring the need for careful adjustment of MgO concentration to achieve desired outcomes. As a result, 7 wt.% MgO emerges as a viable option for balancing CCT uniformity with lumen intensity, offering potential for enhanced LED performance (Royer, 2019; Shih et al., 2020).

The color rendering performance of the LED is further evaluated through the Color Rendering Index (CRI) and Color Quality Scale (CQS) (Shin et al., 2018; My et al., 2022; Tung et al., 2024b). Regarding hue quality evaluation, CRI is said to be the most popular and well-recognized metric. CRI compares the two conditions to ascertain hue quality after evaluating eight hue samples under testing and natural light. One use for CRI is evaluating color performance under wide-spectrum illumination. However, this index cannot be utilized with LED gadgets because it was developed long before they were invented. Using only a few hue samples from CRI would result in extreme desaturation, making it impossible to accurately assess the chromatic output from LED devices. CQS was created to overcome this limitation and generate more precise hue assessments by analyzing fifteen hue samples. In addition to additional hue samples, CQS considers individual preferences and color discrepancy. The color performance of modern devices like LEDs would be better analyzed using CQS, a more current index created in the present day. Figure 5 exhibits the showcases impact of MgO scattering on color reproduction with Figures 5a and 5b illustrating the CRI and CQS, respectively (Ma et al., 2021; Talone and Zibordi, 2020; Tang et al., 2018). The decline in CRI with increasing MgO concentration indicates a shift towards the yellow region due to MgO scattering effects (Wu et al., 2020; Xing et al., 2019; Yang et al., 2021). Conversely, while the CQS gradually decreases with greater MgO concentration, a slight increase is observed at approximately 15 wt.% MgO. This marginal improvement hints at MgO's potential to enhance color reproduction efficiency, particularly at concentrations exceeding 10 wt.%.

Figure 5c displays the changes of acquired spectrum under the concentration of MgO. Apparently, when the MgO concentration changes, LED spectrum also shifts considerably. This means that the scattering-enhancing material MgO greatly influences and benefits the improvement of LED attributes. Ultimately, the study herein makes comparisons between optical parameters of this study and those of earlier studies, which are shown in Table 2 (Le et al., 2024; Anh and Lee, 2024; Tung et al., 2024a; Tung et al., 2024b). In this Table, MgO is compared to four scattering-enhancing materials SiO_2, TiO_2, ZnO and $CaCO_3$. These materials are common and have been assessed in many earlier publications. The study herein would be among the first ones to concern MgO application in LED and there is very little research on this scattering material. Based on comparison results, MgO apparently yields superior results of optical parameters in LED. Notably, when compared to SiO_2, MgO results show a substantial improvement. This would be due to the scattering influences analyzed in Figure 2 and Table 1. The regulation of scattering influences would be done through controlling the MgO concentration added to the phosphor compound. Subsequently, the LED quality can be improved through the method of utilizing scattering materials. The results of this article is a source of valuable reference for LED producers and researchers.

4. CONCLUSIONS

In conclusion, this study demonstrates the significant potential of integrating MgO nanoparticles into yellow phosphor films to enhance the color uniformity and luminous efficiency of conventional white blue-excited LEDs. Through systematic measurement of light scattering across various MgO concentrations within the phosphor layer, utilizing the Mie scattering theory, we have elucidated the role of MgO nanoparticle concentration

in regulating the correlated color temperature (CCT) of white LEDs. Furthermore, the incorporation of MgO nanoparticles enables a reduction in the required amount of yellow phosphor, thereby contributing to cost reduction in LED production. Our findings suggest that MgO concentrations should be carefully selected to optimize specific light properties. For achieving a balance between CCT uniformity and lumen output, a concentration of approximately 7 wt.% MgO proves suitable, while for maximizing lumen output while minimizing backscattering, lower concentrations (<5 wt.%) of MgO are advisable. Additionally, the observed increase in the color quality scale with increasing MgO concentration highlights the potential of MgO scattering features in enhancing white LED performance. Future studies may explore the optimization of MgO nanoparticle utilization through different structural designs, thereby broadening the prospects for its application in LED technology.

5. ACKNOWLEDGEMENT

We would like to thank Prof. Hsiao Yi Lee, from National Kaohsiung University of Science and Technology, in helping to establish this research; and Pham Van De (phamvande@dntu.edu.vn), from Dong Nai Technology University, in contributing to Software, Validation, Investigation, Resources, Data Curation, Review, Visualization.

REFERENCES

Anh, N. D. Q. and H. Y. Lee (2024). Titanium Dioxide in Vanadate Red Phosphor Compound for Conventional White Light Emitting Diodes. *Optoelectronics and Advanced Materials - Rapid Communications*, **18**(9-10); 480–484

Anh, N. D. Q., N. T. P. Loan, P. V. De, and H. Y. Lee (2025). Potassium Bromide Scattering Simulation for Improving Phosphor-Converting White LED Performance. *Optoelectronics and Advanced Materials - Rapid Communications*, **19**(7-8); 378–383

Anh, N. D. Q. and H. V. Ngoc (2020). Building Superior Lighting Properties for WLEDs Utilizing Two-Layered Remote Phosphor Configurations. *Materials Science-Poland*, **38**(3); 493–501

Chen, D., S. Miao, Y. Liang, W. Wang, S. Yan, J. Bi, and K. Sun (2021). Controlled Synthesis and Photoluminescence Properties of Bi_2SiO_5:Eu^{3+} Core-Shell Nanospheres with an Intense 5D0 $\longrightarrow$ 7F4 Transition. *Optical Materials Express*, **11**(2); 355

Cong, P. H. and N. D. Q. Anh (2025). Augmenting Chroma Performance for WLED Employing $Sr_8ZnSc(PO_4)_7$:Eu^{2+}@SiO_2 as a Scattering-Enhancing Substance. *Science and Technology Indonesia*, **10**(2); 467–472

Cong, P. H., L. X. Thuy, N. T. P. Loan, H. Y. Lee, and N. D. Q. Anh (2024). ZnO-Doped Yellow Phosphor Compound for Enhancing Phosphor-Conversion Layer's Performance in White LEDs. *Optoelectronics and Advanced Materials - Rapid Communications*, **18**(7-8); 389–395

Dawodu, A., A. Cheshmehzangi, and A. Sharifi (2020). A Multi-Dimensional Energy-Based Analysis of Neighborhood Sustainability Assessment Tools: Are Institutional Indicators Really Missing? *Building Research and Information*, **49**(5); 574–592

Du, J., Y. An, D. Wu, C. Wang, C. Zhu, X. F. Li, and D. Ma (2020). Easy-to-Process and High-Performance Colorful Perovskite Solar Cells Using a Multilayer Planar Filter. *Optics Letters*, **45**(22); 6326

Fuertes, V., J. F. Fernández, and E. Enríquez (2019). Enhanced Luminescence in Rare-Earth-Free Fast-Sintering Glass-Ceramic. *Optica*, **6**(5); 668

Huang, Z., W. Chen, Q. Liu, Y. Wang, M. R. Pointer, Y. Liu, and J. Liang (2021). Towards an Optimum Color Preference Metric for White Light Sources: A Comprehensive Investigation Based on Empirical Data. *Optics Express*, **29**(5); 6302

Jones, C. M. S., N. A. Panov, E. Hemmer, and J. Marqués-Hueso (2021). Characterizing Up-Conversion Thermometers Through Direct Absolute Photoluminescence Quantum Yield Measurements. In *OSA Optical Sensors and Sensing Congress 2021 (AIS, FTS, HISE, SENSORS, ES)*

Jost, S., C. Cauwerts, and P. Avouac (2018). CIE 2017 Color Fidelity Index Rf: a Better Index to Predict Perceived Color Difference? *Journal of the Optical Society of America*, **35**(4); B202

Le, P. X., N. D. Q. Anh, and H. Y. Lee (2024). Regulating the White LED Properties with Different SiO_2 Particle Sizes. *Optoelectronics and Advanced Materials - Rapid Communications*, **18**(9-10); 485–489

Lee, H., H. Cho, C.-W. Byun, J.-H. Han, B.-H. Kwon, S. Choi, J. Lee, and N. S. Cho (2018). Color-Tunable Organic Light-Emitting Diodes with Vertically Stacked Blue, Green, and Red Colors for Lighting and Display Applications. *Optics Express*, **26**(14); 18351

Li, N., Y. Zhang, Y. Quan, L. Li, S. Ye, Q. Fan, and W. Huang (2018a). High-Efficiency Solution-Processed WOLEDs with Very High Color Rendering Index Based on a Macro-Spirocyclic Oligomer Matrix Host. *Optical Materials Express*, **8**(10); 3208

Li, Y., Y. Wang, E. Y. Pun, and H. Lin (2018b). Bead-on-String Fibers Electro-Spun from Terbium Acetylacetonate Hydrate Doped Poly Methyl Methacrylate. *Optical Materials Express*, **8**(2); 276

Loan, N. T. P., N. D. Q. Anh, N. C. Trang, and H.-Y. Lee (2022). Better Color Distribution Uniformity and Higher Luminous Intensity for LED by Using a Three-Layered Remote Phosphor Structure. *Materials Science Poland*, **40**(1); 60–67

Loan, N. T. P., L. X. Thuy, N. L. Thai, H. Y. Lee, and P. H. Cong (2024). Application of $KBaYSi_2O_7$:Bi^{3+},Eu^{3+} Phosphor for White Light-Emitting Diodes with Excellent Color Quality. *Science and Technology Indonesia*, **9**(3); 756–765

Ma, Y., L. Zhang, J. Huang, R. Wang, T. Li, T. Zhou, Z. Shi, J. Li, Y. Li, G. Huang, Z. Wang, F. A. Selim, M. Li, Y. Wang, and H. Chen (2021). Broadband Emis-

sion $Gd_3Sc_2Al_3O_{12}:Ce^{3+}$ Transparent Ceramics with a High Color Rendering Index for High-Power White LEDs/LDs. *Optics Express*, **29**(6); 9474

My, L. T. T., N. L. Thai, T. M. Bui, H.-Y. Lee, and N. D. Q. Anh (2022). Phosphor Conversion for WLEDs: $YBO_3:Ce^{3+},Tb^{3+}$ and Its Effects on the Luminous Intensity and Chromatic Properties of Dual-Layer WLED Model. *Materials Science Poland*, **40**(4); 105–113

Peng, Y., Y. Mou, X. Guo, X. Xu, H. Li, and X. Luo (2018). Flexible Fabrication of a Patterned Red Phosphor Layer on a YAG:Ce^{3+} Phosphor-in-Glass for High-Power WLEDs. *Optical Materials Express*, **8**(3); 605

Royer, M. P. (2019). Evaluating Tradeoffs Between Energy Efficiency and Color Rendition. *OSA Continuum*, **2**(8); 2308

Shih, H.-K., C.-N. Liu, W.-C. Cheng, and W.-H. Cheng (2020). High Color Rendering Index of 94 in White LEDs Employing Novel $CaAlSiN_3:Eu^{2+}$ and $Lu_3Al_5O_{12}:Ce^{3+}$ Co-Doped Phosphor-in-Glass. *Optics Express*, **28**(19); 28218

Shin, J.-Y., H. Cho, J. Lee, J. Moon, J.-H. Han, K. Kim, S. Cho, J.-I. Lee, B.-H. Kwon, D.-H. Cho, K. M. Lee, M. Suemitsu, and N. S. Cho (2018). Overcoming the Efficiency Limit of Organic Light-Emitting Diodes Using Ultra-Thin and Transparent Graphene Electrodes. *Optics Express*, **26**(2); 617

Talone, M. and G. Zibordi (2020). Spatial Uniformity of the Spectral Radiance by White LED-Based Flat-Fields. *OSA Continuum*, **3**(9); 2501

Tang, W., B. Wang, Y. Chen, Y. Chen, J. Lin, and Q. Zeng (2018). Single Pr^{3+}-Activated High-Color-Stability Fluoride White-Light Phosphor for White-Light-Emitting Diodes. *Optical Materials Express*, **9**(1); 223

Thi, M. H. N., P. T. That, and N. D. Q. Anh (2020a). Eu^{2+}-Activated Strontium-Barium Silicate: a Positive Solution for Improving Luminous Efficacy and Color Uniformity of White Light-Emitting Diodes. *Materials Science-Poland*, **38**(4); 594–600

Thi, M. H. N., P. T. That, N. D. Q. Anh, and T. T. Trang (2020b). Triple-Layer Remote Phosphor Structure: a Novel Option for the Enhancement of WLEDs' Color Quality and Luminous Flux. *Materials Science Poland*, **38**(4); 654–660

Tung, H. T., N. D. Q. Anh, and H. Y. Lee (2024a). Impact of Phosphor Granule Magnitudes as well as Mass Proportions on the Luminous Hue Efficiency of a Coated White Light-Emitting Diode and one Green Phosphor Film. *Optoelectronics and Advanced Materials - Rapid Communications*, **18**(1-2); 58–65

Tung, H. T., B. T. Minh, N. L. Thai, H. Y. Lee, and N. D. Q. Anh (2024b). ZnO Particles as Scattering Centers to Optimize Color Production and Lumen Efficiencies of Warm White LEDs. *Optoelectronics and Advanced Materials - Rapid Communications*, **18**(5-6); 1–6

Wu, C., Z. Liu, Y. Zhi-Guo, X. Peng, Z. Liu, X. Liu, X. Yao, and Y. Zhang (2020). Phosphor-Converted Laser-Diode-Based White Lighting Module with High Luminous Flux and Color Rendering Index. *Optics Express*, **28**(13); 19085

Xing, Y., C. Chai, J. Chen, S. Zheng, and C. Chen (2019). Single 395 nm Excitation Warm WLED with a Luminous Efficiency of 10486 lm/W and a Color Rendering Index of 907. *Optical Materials Express*, **9**(11); 4273

Yang, H., P. Li, Z. Ye, X. Huo, Q. Wu, Y. Wang, and Z. Wang (2021). Structural Modulation Designed a Thermally Robust Blue-Cyan Emitting Phosphor $Y_2Mg_{0\cdot 8}Sr_{0\cdot 2}Al_4SiO_{12}:Eu^{2+}$ for the High Color Rendering Index White LEDs. *Optics Letters*, **46**(22); 5639

Zhang, W., W. Yang, P. Zhong, S. Mei, G. Zhang, G. Chen, G. He, and R. Guo (2017). Spectral Optimization of Color Temperature Tunable White LEDs Based on Perovskite Quantum Dots for Ultrahigh Color Rendition. *Optical Materials Express*, **7**(9); 3065

Zhong, W., J. Liu, D. Hua, S. Guo, K. Yan, and C. Zhang (2019). White LED Light Source Radar System for Multi-Wavelength Remote Sensing Measurement of Atmospheric Aerosols. *Applied Optics*, **58**(31); 8542

